

Distribution of Gallium Nanocrystals in Ga/MCM-41 Mesocomposites by Continuous-Flow Hyperpolarized ^{129}Xe NMR Spectroscopy

Weiping Zhang,^{*,†,‡} Christopher I. Ratcliffe,[†] Igor L. Moudrakovski,[†] Chung-Yuan Mou,[§] and John A. Ripmeester[†]

Steele Institute for Molecular Sciences, National Research Council of Canada, 100 Sussex Drive, Ottawa, Ontario K1A 0R6, Canada, State Key Laboratory of Catalysis, Dalian Institute of Chemical Physics, Chinese Academy of Sciences, Dalian 116023, China, and Department of Chemistry and Center of Condensed Matter Research, National Taiwan University, Taipei, Taiwan

The distribution of gallium nanocrystals in mesoporous MCM-41 host were analyzed by continuous-flow hyperpolarized ^{129}Xe NMR spectroscopy. In contrast to unclear TEM images for the high metal contents, laser-polarized ^{129}Xe probe can detect the whole distribution of gallium in the MCM-41 host. It is found that gallium nanocrystals are included in the mesochannels of MCM-41; a part of them also remains in the interparticle voids. The distribution of gallium metal in MCM-41 is heterogeneous. Not all the mesochannels host metallic gallium even at a high gallium loading of 65.1 wt %. Variable temperature measurements can provide information on the xenon adsorption parameters. This approach opens a sensitive way to probe the distribution of high content species in porous host materials.

The structure and performance of metal and semiconductor nanocrystals in confined spaces are the subject of continuing interest because they are significantly different from those in the corresponding bulk substances and have various potential applications in optical, electrical devices and sensors.^{1,2} Mesoporous silica MCM-41 has the regular array of cylindrical channels with controllable mesopore size distribution.³ The absence of pore channel interactions in MCM-41 guarantees that the pore networking effects are negligibly small. Recent studies have shown that this mesoporous material is a mostly suitable model adsorbent to host the semiconductor nanocrystals such as gallium inside.⁴ Probably, the most direct means of demonstrating the location of nanocrystals in the mesoporous host would be transmission electron microscopy (TEM); however, attempts to obtain clear

TEM images were unsuccessful due to high metal loadings in metal/SBA-15 (MCM-41) nanocomposites.^{4b} ^{129}Xe NMR spectroscopy has been widely used for probing the nanometer-scaled void spaces and species distribution in porous solids because small variations in the physical interactions between xenon and the neighboring environment cause marked perturbations of its extremely polarizable electron cloud, which are transferred directly to the xenon nucleus and greatly affect the NMR chemical shift.^{5–7} In porous silica without strong adsorption sites, the ^{129}Xe NMR chemical shift can be expressed as a sum of three main contributions: $\delta = \delta_0 + \delta_s + \delta_{\text{Xe-Xe}}$. Here δ_0 is the reference shift, which is usually set to 0 ppm, the chemical shift of xenon gas at zero pressure. δ_s is the contribution due to the interaction of Xe with the surface, and $\delta_{\text{Xe-Xe}}$ is the contribution from Xe–Xe interactions.^{5,6} However, the application of thermally polarized ^{129}Xe NMR to materials has been hampered by the low concentration of adsorbed xenon, dynamically averaged chemical shifts among different xenon environments, and long relaxation times (this is particularly the case for amorphous materials such as mesoporous silica⁸). The use of optical pumping techniques for production of hyperpolarized (HP) xenon can increase sensitivity of several orders of magnitude ($\times 10^4$).⁹ This technique works at very low concentrations of xenon ($\sim 1\%$) under continuous flow, the contribution of Xe–Xe interactions is rather insignificant at ambient temperature, and the observed ^{129}Xe chemical shift could reflect mainly the interactions between xenon atoms and the surface, i.e., the chemical composition of the surface and geometry of the xenon environment in that particular site. These have made it very attractive for materials analysis¹⁰ and allowed very small quantities of samples to be probed.¹¹ In this study, the continuous-flow HP ^{129}Xe NMR technique is used to analyze the pore structures of mesoporous materials confined with Ga nanocrystals. The distribution of metallic Ga in Ga/MCM-41 nanocomposites

* Corresponding author. Fax: 86-411-84694447. E-mail: wpzhang@dicp.ac.cn.

[†] Steele Institute for Molecular Sciences.

[‡] Dalian Institute of Chemical Physics.

[§] National Taiwan University.

(1) Alivisatos, A. P. *Science* **1996**, *271*, 933–937.

(2) Hu, J.; Odom, T. W.; Lieber, C. M. *Acc. Chem. Res.* **1999**, *32*, 435–445.

(3) Kresge, C. T.; Leonowicz, M. E.; Roth, W. J.; Vartuli, J. C.; Beck, J. S. *Nature* **1992**, *359*, 710–712.

(4) (a) Srdanov, V. I.; Alkeit, I.; Stucky, G. D.; Reaves, C. M.; DenBaars, J. *Phys. Chem. B* **1998**, *102*, 3341–3344. (b) Han, Y. J.; Kim, J. M.; Stucky, G. D. *Chem. Mater.* **2000**, *12*, 2068–2069. (c) Charnaya, E. V.; Tien, C.; Lin, K. J.; Kumzerov, Y. A. *Phys. Rev. B* **1998**, *58*, 11089–11092.

(5) Ratcliffe, C. I. *Annu. Rep. NMR Spectrosc.* **1998**, *36*, 123–221.

(6) Bonardet, J. L.; Fraissard, J.; Gedeon, A.; Springuel-Huet, M. A. *Catal. Rev.-Sci. Eng.* **1999**, *41*, 115–225.

(7) Zhang, W.; Han, X.; Liu, X.; Lei, H.; Bao, X. *Chem. Commun.*, **2001**, 293–294.

(8) Pietrass, T.; Kneller, J. M.; Assink, R. A.; Anderson, M. T. *J. Phys. Chem. B* **1999**, *103*, 8837–8841.

(9) Happer, W.; Miron, E.; Schaefer, S.; Schreiber, D.; van Wingen, W. A.; Zeng, X. *Phys. Rev. A* **1984**, *29*, 3092–3110.

is described for the first time using HP ^{129}Xe NMR spectroscopy at high gallium loadings.

EXPERIMENTAL SECTION

Mesoporous MCM-41 host was prepared according to the procedures reported in our previous study using cetyltrimethylammonium bromide as the structure-directing agent.¹² The resultant MCM-41 samples have the typical hexagonal structure and BET surface area of 1104 m²/g after calcinations at 823 K for 8 h.^{12a} Before introducing metallic Ga, MCM-41 samples were degassed at 423 K under vacuum. A measured amount of gallium (purity 99.99%, Strem Chemicals) was added under high-purity nitrogen atmosphere. The mixture was stirred at 313 K for ~2 h until a homogeneous sample was obtained, and then it was heated to 573 K at 2 K/min under vacuum ($<10^{-2}$ Pa) and held under these conditions for 8 h. The obtained Ga/MCM-41 composites are gray to black depending on the gallium loadings and are denoted as $x\text{Ga}/\text{M}-41$, where x is the weight percentage of metallic gallium. Because the melting point of metallic Ga is 29.9 °C at 1 atm,¹³ it can diffuse into the channels of MCM-41 upon heating and evacuation. Partial pore filling of the host MCM-41 is demonstrated by a decrease of pore volume and surface area of MCM-41 after introduction of Ga.^{12a}

^{129}Xe NMR experiments were carried out at 83.03 MHz on a Bruker AMX-300 spectrometer using a 10-mm static probe (Morris Instrument Inc.). Samples were heated at 383 K in situ under helium flow to remove adsorbed water and gas prior to delivery of hyperpolarized xenon. Optical polarization of xenon was achieved with an apparatus similar to that in ref 14, with the optical pumping cell in the fringe field of the spectrometer magnet and diode laser array. A flow of 1% Xe–1% N₂–98% He gas mixture was delivered at the rate of 200–250 cm³/min to the sample in the detection region via plastic tubing. Variable temperature NMR measurements were also performed in the range of 173–363 K with this probe using a Bruker BVT3000 temperature controller. All the spectra were acquired with 8.5- μs $\pi/2$ pulse, 64 scans, and 1-s recycle delay, which was found to be sufficient to avoid saturation of the signal at the flow rate of gas mixture used. The chemical shifts were referenced to the signal of xenon gas.

RESULTS AND DISCUSSION

Variations in the ^{129}Xe NMR spectra with temperature can be very sensitive to the dynamics of adsorbed xenon and subsequently to the pore structure and species distribution. By performing variable temperature ^{129}Xe NMR measurements, it is possible to distinguish xenon in the micropore and mesopore regions and

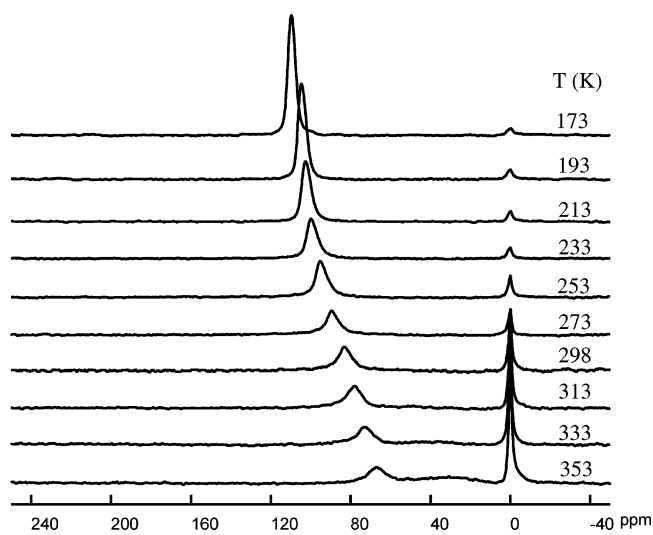


Figure 1. Variable temperature continuous-flow hyperpolarized ^{129}Xe NMR spectra of mesoporous MCM-41 host.

obtain heats of adsorption.^{10c,15} Figure 1 shows the variable temperature continuous-flow HP ^{129}Xe NMR spectra of mesoporous MCM-41 host. The peak at 0 ppm in the spectra is from xenon in the gas phase. All signals at lower field are originated from the adsorbed xenon. At 353 K, the sharp line above 60 ppm is attributed to xenon in the primary mesochannels of MCM-41, while the broad line centered at ~30 ppm is ascribed to xenon in larger secondary pores such as interparticle voids.¹⁵ The decrease of the temperature leads to a reduction of the peak intensity of gas xenon, while increases the signal of adsorbed xenon in the mesochannels of MCM-41 and shifts the signal to the lower field. This can be due to the fact that more and more xenon in the gas phase will be condensed in the samples at lower temperatures, which increases the xenon–xenon interactions in the adsorbed state even at low partial pressures of xenon. Moreover, the line of xenon in the interparticle pores of MCM-41 is not observed notably at lower temperatures except in its primary mesochannels. This demonstrates that the capillary condensation of xenon preferentially takes place in the primary mesochannels of MCM-41 instead of its interparticle pores at lower temperatures. The line width of the signal related to xenon in the mesochannels decreases with decreasing temperatures; this may be due to the longer relaxation time of xenon as the temperature goes down.

After introducing gallium inside MCM-41, the continuous-flow HP ^{129}Xe NMR spectra of Ga/MCM41 nanocomposites at certain temperatures are shown in Figure 2. At room temperature of 298 K (Figure 2b), the peak intensity of xenon at ~80 ppm in the mesocomposites decreases with increasing gallium loading from 18.6 to 65.1 wt %, and its chemical shift is nearly consistent with that in the primary mesochannels of MCM-41. Meanwhile, a new signal at ~100 ppm appears in the lower field. This larger chemical shift is still in the range of mesopores.¹⁶ It becomes sharper and stronger at lower temperatures of 233 and 193 K (Figure 2c,d), and its intensity increases gradually at the expense of the proximal signal at higher field with increasing gallium loadings. On the

(10) (a) Haake, M.; Pines, A.; Reimer, J. A.; Seydoux, R. *J. Am. Chem. Soc.* **1997**, *119*, 11711–11712. (b) Moudrakovski, I. L.; Nossov, A.; Lang, S.; Breeze, S. R.; Ratcliffe, C. I.; Simard, B.; Santyr, G.; Ripmeester, J. A. *Chem. Mater.* **2000**, *12*, 1181–1183. (c) Nossov, A.; Haddad, E.; Guenneau, F.; Galarneau, A.; Di Renzo, F.; Fajula, F.; Gedeon, A. *J. Phys. Chem. B* **2003**, *107*, 12456–12460.

(11) Dubes, A.; Moudrakovski, I. L.; Shahgaldian, P.; Coleman, A. W.; Ratcliffe, C. I.; Ripmeester, J. A. *J. Am. Chem. Soc.* **2004**, *126*, 6236–6237.

(12) (a) Zhang, W.; Ratcliffe, C. I.; Moudrakovski, I. L.; Tse, J.; Mou, C.-Y.; Ripmeester, J. A. *Microporous Mesoporous Mater.* **2005**, *79*, 195–203. (b) Du, H.; Tersikh, V. V.; Ratcliffe, C. I.; Ripmeester, J. A. *J. Am. Chem. Soc.* **2002**, *124*, 4216–4217.

(13) Lide, D. R., Ed. *CRC Handbook of Chemistry and Physics*, 82nd ed.; CRC Press Inc.: Boca Raton, FL, 2001.

(14) Brunner, E.; Seydoux, R.; Haake, M.; Pines, A.; Reimer, J. A. *J. Magn. Reson.* **1998**, *130*, 145–148.

(15) Moudrakovski, I. L.; Tersikh, V. V.; Ratcliffe, C. I.; Ripmeester, J. A.; Wang, L.; Shin, Y.; Exarhos, G. J. *J. Phys. Chem. B* **2002**, *106*, 5938–5946.

(16) Moudrakovski, I. L.; Wang, L.; Baumann, T.; Satcher, J. H.; Exarhos, G. J.; Ratcliffe, C. I.; Ripmeester, J. A. *J. Am. Chem. Soc.* **2004**, *126*, 5052–5053.

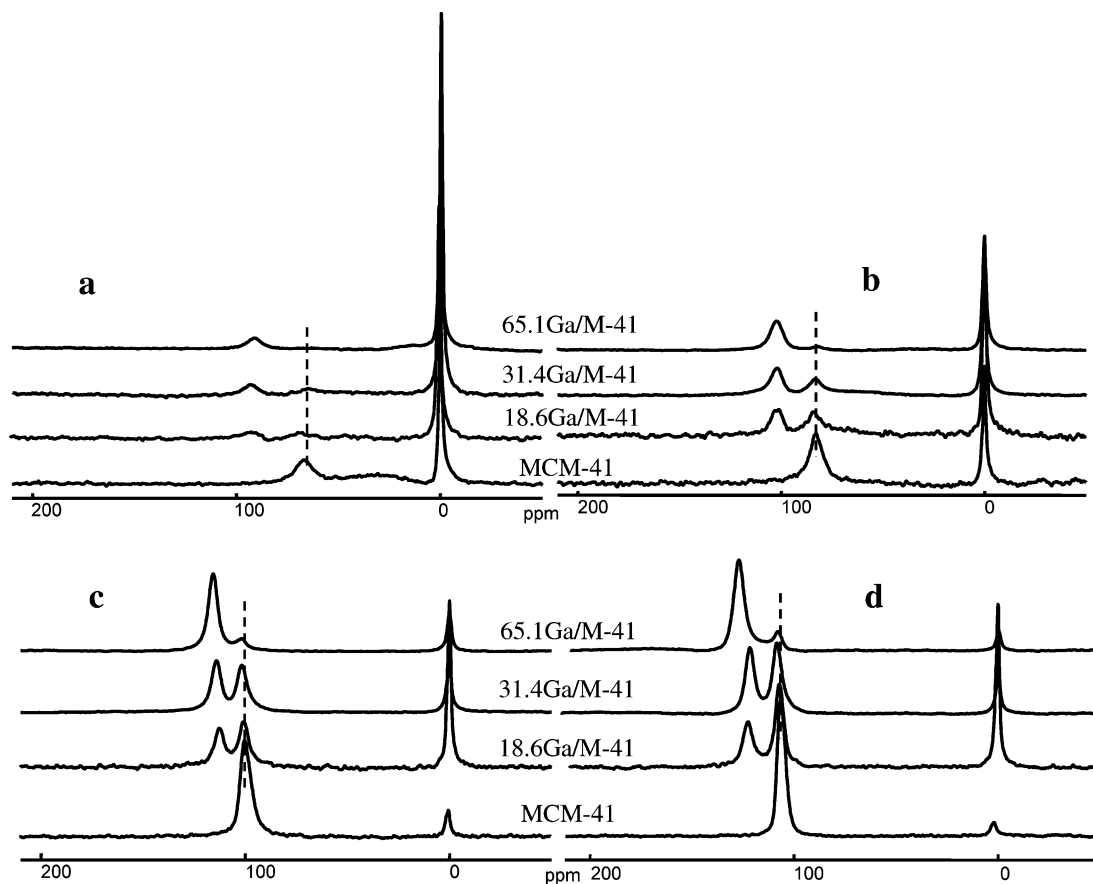


Figure 2. Continuous-flow hyperpolarized ^{129}Xe NMR spectra of Ga/MCM-41 mesocomposites at different temperatures: (a) 353, (b) 298, (c) 233, and (d) 193 K.

basis of these facts, we attribute the signal at higher field in Figure 2b–d to xenon in the empty mesochannels of MCM-41, and the new proximal signal at lower field to xenon in the mesochannels of MCM-41 hosting gallium nanocrystals. Figure 2 also indicates that more and more gallium will be introduced into the mesochannels of MCM-41 with increasing loadings. For example, at a gallium loading of 65.1 wt %, the low-field signal is much stronger than the proximal high-field signal. This means that gallium nanocrystals will be distributed in most mesochannels of MCM-41, and the residual empty mesochannels are less in this sample. However, in Figure 2a acquired at higher temperatures (353 K), the broad signal of xenon in the interparticle voids at ~ 30 ppm decreases with introduction of gallium inside MCM-41. This indicates that a part of metallic gallium is also distributed in the interparticle spaces.

The temperature-dependent Xe chemical shifts in the MCM-41 mesochannels containing gallium nanocrystals are displayed in Figure 3. At each temperature, the chemical shifts of Xe (δ_s) in Ga/MCM-41 mesocomposites are much higher than in MCM-41 host. This indicates the shorter average free path of xenon (λ) in the mesocomposites as derived from the correlation of $\delta_s = A/(B + \lambda)$, where A and B are empirical constants.¹⁷ So, gallium is included in the mesochannels of MCM-41, which shortens the channel lengths of MCM-41. For the Ga/MCM-41 mesocomposites, the chemical shifts are very close at temperatures higher than 298 K, but they increase gradually with

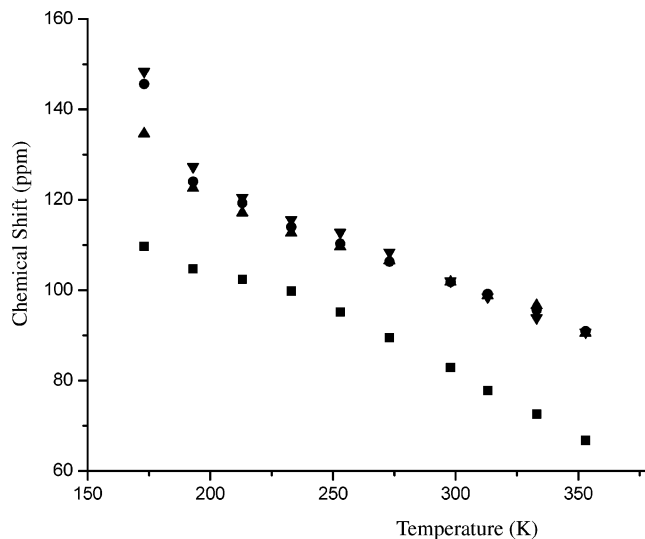


Figure 3. Temperature-dependent ^{129}Xe NMR chemical shifts of the resonance line of xenon adsorbed in the mesochannels of MCM-41 containing Ga nanocrystals: (■) MCM-41 host, (▲) 18.6 Ga, (●) 31.4 Ga, and (▼) 65.1 Ga.

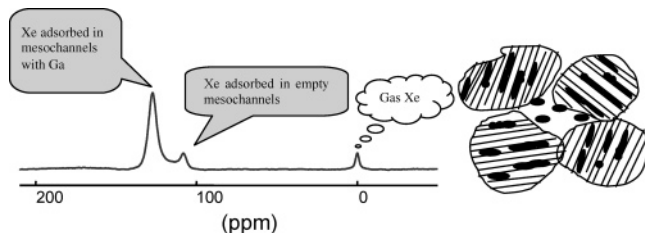
increasing gallium loadings at each temperature below 298 K. This suggests that the fast exchange processes among xenon in the empty mesochannels, mesochannels containing gallium nanocrystals, interparticle voids, and gas phase average the chemical shifts at higher temperatures. But these exchange processes slow in the lower temperature region, so the channel lengths of the MCM-41 host have great effect on the xenon chemical shifts at

(17) Demarquay, J.; Fraissard, J. *Chem. Phys. Lett.* **1987**, *136*, 314–318.

Table 1. Heats of Xenon Adsorption in Ga/MCM-41 Nanocomposites

sample	heat of adsorption (kJ/mol)
MCM-41	8.4 ± 0.8
18.6Ga/M-41	5.6 ± 0.5
31.4Ga/M-41	5.2 ± 0.5
65.1Ga/M-41	5.7 ± 0.6

Chart 1. Porous Structure and Ga Nanocrystals Distribution in MCM-41 Described by Hyperpolarized ^{129}Xe NMR Spectroscopy



low temperatures. As seen from Figure 3, the ^{129}Xe chemical shifts increase gradually with increasing gallium loadings at each low temperature. This also indicates the shorter channel lengths of MCM-41 after hosting more and more gallium nanocrystals.

Assuming only the weak adsorption of xenon has taken place, as described by Henry's law, quantitative information on xenon adsorption can be extracted. The temperature dependence of the observed xenon chemical shift δ for cylindrical pores can be expressed as¹⁵

$$\delta = \delta_s \left(1 + \frac{D}{4K_0RT^{1/2} \exp(\Delta H_{\text{ads}}/RT)} \right)^{-1} \quad (1)$$

where K_0 is the pre-exponent in the Henry equation, D is the channel diameter, R is the universal gas constant, ΔH_{ads} is the heat of adsorption, and δ_s is the ^{129}Xe chemical shift characteristic

of the surface. Linearization of this equation leads to

$$\ln[(\delta_s/\delta - 1)T^{1/2}] = \ln(D/4K_0R) - \Delta H_{\text{ads}}/RT \quad (2)$$

By fitting the temperature-dependent data given in Figure 3 with eq 2, one can determine the heat of xenon adsorption ΔH_{ads} by plotting $\ln[(\delta_s/\delta - 1)T^{1/2}]$ versus T^{-1} and by using the value of $\delta_s = 116$ ppm, which is characteristic of the silica surface.¹⁸ The obtained ΔH values are listed in Table 1. The xenon adsorption heat decreases as gallium nanocrystals are introduced inside the mesochannels of MCM-41. These values are in the same range as those previously obtained for other silica samples,^{10c,15} which indicates a process of typical physical adsorption.

CONCLUSIONS

As described in Chart 1, we have demonstrated the capability of continuous-flow hyperpolarized ^{129}Xe NMR to analyze the pore structure and distribution of gallium nanocrystals in Ga MCM-41 mesocomposites with high metal loadings. In contrast to TEM, a laser-polarized ^{129}Xe probe can detect the whole region of the sample and provide the overall distribution of gallium in the MCM-41 host. With increasing Ga loadings, more and more gallium is introduced into the mesochannels of MCM-41, and a portion of gallium remains in the interparticle voids. There are still empty mesochannels left even at high gallium loading of 65.1 wt %, which indicates the distribution of gallium nanocrystals in MCM-41 is heterogeneous. The adsorption heat evaluated from the variations of ^{129}Xe chemical shift with the temperature reveals a physical adsorption of xenon in Ga/MCM-41 mesocomposites. This approach opens a sensitive way to probe the distribution of high content species in porous host materials.

Received for review January 14, 2005. Accepted March 17, 2005.

AC050076J

(18) Terskikh, V. V.; Moudrakovski, I. L.; Breeze, S. R.; Lang, S.; Ratcliffe, C. I.; Ripmeester, J. A.; Sayari, A. *Langmuir* 2002, 18, 5653–5656.